View Article Online
View Journal

Faraday Discussions

Accepted Manuscript

This manuscript will be presented and discussed at a forthcoming Faraday Discussion meeting.
All delegates can contribute to the discussion which will be included in the final volume.

Register now to attend! Full details of all upcoming meetings: http://rsc.li/fd-upcoming-meetings

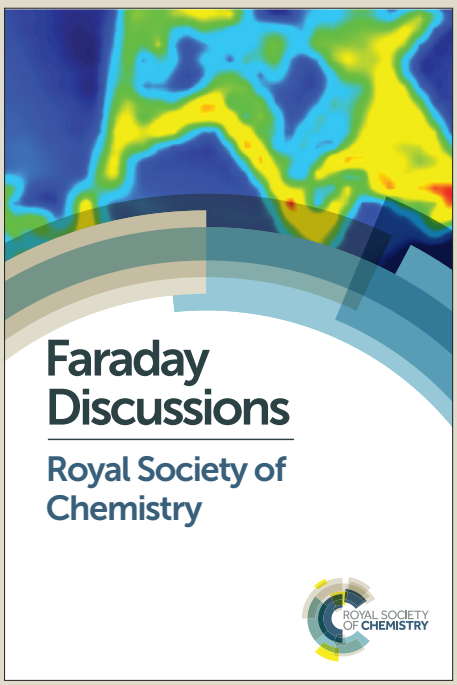

This is an *Accepted Manuscript*, which has been through the Royal Society of Chemistry peer review process and has been accepted for publication.

Accepted Manuscripts are published online shortly after acceptance, before technical editing, formatting and proof reading. Using this free service, authors can make their results available to the community, in citable form, before we publish the edited article. We will replace this *Accepted Manuscript* with the edited and formatted *Advance Article* as soon as it is available.

You can find more information about *Accepted Manuscripts* in the Information for Authors.

Please note that technical editing may introduce minor changes to the text and/or graphics, which may alter content. The journal's standard Terms & Conditions and the Ethical guidelines still apply. In no event shall the Royal Society of Chemistry be held responsible for any errors or omissions in this *Accepted Manuscript* or any consequences arising from the use of any information it contains.

This article can be cited before page numbers have been issued, to do this please use: K. Bennett, M. Kowalewski and S. Mukamel, *Faraday Discuss.*, 2014, DOI: 10.1039/C4FD00178H.

ROYAL SOCIETY OF CHEMISTRY

www.rsc.org/faraday_d

View Article Online
DOI: 10.1039/C4FD00178H

Probing Electronic and Vibrational Dynamics in Molecules by Time-Resolved Photoelectron, Auger-Electron, and X-ray Photon Scattering Spectroscopy

Kochise Bennett,* Markus Kowalewski, and Shaul Mukamel†
Chemistry Department, University of California, Irvine, California 92697-2025, USA
(Dated: September 17, 2014)

We present a unified description for time-resolved electron and photon scattering spectroscopies from molecules prepared in nonstationary states. Signals are expressed in terms of superoperator Green's functions and a systematic procedure for treating various degrees of freedom consistently at different levels of theory is developed. The standard Fermi Golden Rule expressions for photelectron spectra, which are limited to broad, slowly-varying signals, are obtained as a limiting case of our more general theory that applies to broader parameter regimes.

Published on 04 November 2014. Downloaded by University of California - Irvine on 04/11/2014 18:23:19.

Faraday Discussions Accepted Manuscript

* kcbennet@uci.edu
† smukamel@uci.edu

View Article Online
DOI: 10.1039/C4FD00178H

Published on 04 November 2014. Downloaded by University of California - Irvine on 04/11/2014 18:23:19.

I. INTRODUCTION

Molecular photophysical processes are widely monitored by detecting ejected electrons or scattered X-ray photons [1–4]. We present a computational framework for time-resolved photoelectron spectroscopy (TRPES), Auger-electron spectroscopy (AES), and off-resonant X-ray scattering (OXS). In these experiments, the common objective is to monitor the electronic and nuclear dynamics of nonstationary states (often prepared by excitation with a pump pulse). Electron spectroscopies in the X-ray regime will depend on valence, core, and continuum electronic states, and nuclear degrees of freedom as well as fluctuations from coupling to the environment (this could be a thermal bath or represent solvent degrees of freedom). Often, exactly including the nuclei quantum mechanically is numerically too expensive and the Born-Oppenheimer approximation is made (separation of electronic and nuclear degrees of freedom). Of course, this sepration fails when electronic modes are vibronically coupled or as at degeneracies (conical intersections)[5, 6]. Thus, the level of theory employed for the nuclei can vary greatly (e.g., harmonic oscillators, brownian oscillators, averaging over semiclassical trajectories, sufrace hopping, spawning [7]). In particular, if some nuclear degrees of freedom can be identified as the origin of the strongest intramolecular interactions and fastest dynamics, it would be preferable to treat these explicitly. The remaining nuclear modes can then be treated implicitly (such an approach was advocated by Seel and Domcke for TRPES[8]). Except for model systems in which such effects can be explicitly included in the Hamiltonian and solved analytically, they are normally treated by numerical propagation or modification to the Fermi Golden Rule (FGR). The many choices of what level of theory to employ for various degrees of freedom calls for a consistent and comprehensive approach to these signals. Liouville space is a natural setting for handling bath degrees of freedom and making semiclassical approximations and it therefore provides a unified treatment of these experiments.

We start with time-resolved photoelectron spectroscopy (TRPES) which is a pump-probe technique in which a pump pulse prepares the system and, after some controlled delay time, a probe pulse ionizes it [1]. The photoelectron current is generally plotted as a function of the pulse parameters (principally the interpulse delay) and the kinetic energy of the photoelectrons. The photelectron energy is given bythe difference in energy between the ionized and unionized system. Comparison with the ground state spectra can thus be used to analyze the electronic and vibrational excited state dynamics and to monitor non-radiative decay channels. Photoelectron spectroscopy has been utilized to study a wide variety of material systems (e.g. atoms, molecules, films and surfaces, and metals [9–12]) and has recently been used to track the non-adiabatic radationless decay of various organic molecules (e.g. uracil, thymine, benzene, and cis-dienes [13–15]) complementing optical methods (e.g. [16]). TRPES has simplified selection rules compared to optical detection schemes (any orbital may be ionized and the transition dipole to the continuum states does not depend much on the continuum state and may be well-approximated as flat in certain regions). The probabilities for excitation to various continuum states can still depend sensitively on the final molecular electronic state and one can therefore use knowledge of the continuum states as a probe [1, 8].

In the X-ray regime, the TRPES process involves valence, core, and continuum electronic states. Photoionization prepares a core hole state, whose dynamics can be studied. In particular, this state ordinarily rapidly decays as a valence electron fills the core hole while a second valence electron (the Auger electron, which is the object of study in AES) is ejected with kinetic energy equal to the core-valence energy gap. Besides being of interest in studying core-hole dynamics (the Auger decay process adds a linewidth to the TRPES spectra), the Auger process is governed by a Coulomb matrix element rather than a transition dipole. This difference in selection rules often leads to broader, less distinct spectra but can be useful in viewing dipole-forbidden transitions. Like TRPES, AES has been used to study the dynamics for diatomics, biomolecules, metals, oxide films, and electrolytes,[8, 9, 11, 17–19]. Because of the complexity of these processes, a variety of approaches have been taken for their simulation including methods based on direct wavefunction propagation, many-body non-equilibrium Green's functions and the core-hole spectral function as well as a more straightforward quadratic-response function formalism [20–24]. While these are frequently approximated in a "two-step" fashion in which the photoionization event is separated from the Auger decay (the ionization is also typically taken to be to the relaxed core-hole state), removing these restrictions is necessary to describe gain-loss peaks in the Auger spectra due to excited states induced by the ionization process [25, 26]. Such considerations are obviously important when tracking the decay of electronic excited states via TRPES/AES and, in this paper, we employ a one-step description so that the entire history of the system is properly included.

A third commonly employed technique for tracking the structure and dynamics of materials is the detection of scattered, off-resonant X-rays, whose elastic portion, diffraction, has been widely used to study the electronic charge density of materials [3, 4, 27–29]. In a recent paper, we examined time-, frequency-, and wavevector-resolved OXS from non-stationary states and found that, under certain assumptions, the signal separates into one- and two-particle terms which carry different form factors [30]. For OXS from the ground state, the two-particle form factor was found to contain only elastic contributions while all inelastic processes were contained in the one-particle form factor. The inelastic contributions are thus dominated by the elastic for a many-particle sample. The one-particle form factor contains many inelastic terms and is clearly the only contribution in a single molecule experiment. These inelasticities

Faraday Discussions Accepted Manuscript

View Article Online
DOI: 10.1039/C4FD00178H

Published on 04 November 2014. Downloaded by University of California - Irvine on 04/11/2014 18:23:19.

are therefore expected to be especially relevant for ultrafast diffraction from single-molecules, a regime that has drawn considerable interest recently[31–34].

In this paper, we recast the theory of TRPES and AES in Liouville space; a previous treatment incorporated multidimensional processes and quantum fields but did not explicitly consider vibronic couplings between electronic states [35]). From this, we derive the FGR expression ordinarily associated with these signals showing the assumptions required along the way. The FGR should not hold when the nuclear dynamics is fast compared to the photoionization time. We thus expect it to break down near conical intersections where a more general formula will be needed. Following exposition of the Liouville space formalism, we provide a semiclassical simulation of the TRPES signal from acroleine following preparation of a valence excitation and discuss how this simulation procedure may be generalized to allow for nuclear motion during electronic coherences. We then discuss the case of OXS as recently recast so as to explicitly include the time, frequency, and wavevector resolution of the photon detection event and analogies to TRPES/AES are discussed. In particular, all of these processes, in addition to being useful probes of nonstationary states at both the electronic and nuclear level, prepare interesting states in their own right. That is, following these processes, the system is left in another nonstationary excited state. This state may then be probed by other nonlinear spectroscopic measurements and the Liouville space theory presented herein is easily adapted to describe these further considerations.

II. PHOTOELECTRON SPECTROSCOPY; HAMILTONIAN AND THE FERMI GOLDEN RULE

We describe TRPES with the following Hamiltonian:

$$H = H_{\rm M} + H_{\mathbf{p}} + H_{\rm x}(t) + H_{\rm v}(t) \tag{1}$$

where

$$H_{\rm M} = \sum_{II'{\rm q}} |I_{\rm q}\rangle \mathcal{E}_{I_{\rm q}} \langle I_{\rm q}| + |I'_{\rm q}\rangle H_{I'I} \langle I_{\rm q}| \tag{2}$$

represents the molecule with $\mathcal{E}_{I_{\rm q}}$ the energy of the I-th electronic state with q holes and $H_{I'I}$ the coupling between electronic states via nuclear coordinates. Both are therefore operators in the nuclear subspace. In a fully microscopic theory, the states and parameters would be given in terms of single-particle occupation numbers (in a second-quantized representation). This is discussed further in the appendix but for now, we only treat the continuum electrons in this manner.

$$H_{\mathbf{p}} = \sum_{\mathbf{p}} \varepsilon_{\mathbf{p}} c^\dagger_{\mathbf{p}} c_{\mathbf{p}} \tag{3}$$

is the Hamiltonian of the photoelectron states ($c^\dagger_{\mathbf{p}}, c_{\mathbf{p}}$ are creation/annihilation operators for the orbital with energy $\varepsilon_{\mathbf{p}}$) and $H_{\rm x}(t)$, $H_{\rm v}(t)$ are the Hamiltonians for interactions with photoionizing x-ray and valence pump fields respectively. We assume that $H_{\rm M}$ is block diagonal in the molecular charge number and label electronic states of $H_{\rm M}$ as $|I_{\rm q}\rangle$ where the subscript indicates the molecular charge. The molecular Hamiltonian remains an operator in the nuclear subspace while we assume that the Hamiltonian of the continuum states is independent of the nuclei. In the simplest model, the nuclear coupling gives a vibrational splitting to each electronic state. More generaly, the nuclear degrees of freedom can couple the electronic states (as in surface crossing and non-Born-Oppenheimer effects) leading to population transport, etc. In the Condon approximation, the dipolar interaction with the valence pump pulse is

$$H_{\rm v}(t) = -E_{\rm v}(t) \sum_{II'} \mu^{({\rm q})}_{I'I} |I'_{\rm q}\rangle\langle I_{\rm q}| + \mu^{({\rm q})*}_{I'I} |I_{\rm q}\rangle\langle I'_{\rm q}| \tag{4}$$

where $E_{\rm v}(t)$ is the temporal envelope of the valence pump pulse. We work in the product space of bound and continuum states and interaction with the photoionizing X-ray pulse is then written as

$$H_{\rm x}(t) = -E_{\rm x}(t) \sum_{II'\mathbf{p}} \mu^{({\rm q})}_{\mathbf{p}I'I} c^\dagger_{\mathbf{p}} |I'_{\rm q+1}\rangle\langle I_{\rm q}| + \mu^{({\rm q})*}_{\mathbf{p}I'I} c_{\mathbf{p}} |I_{\rm q}\rangle\langle I'_{\rm q+1}| \tag{5}$$

where $E_{\rm x}(t)$ is the temporal envelope of the ionizing X-ray pulse and we have explicitly indicated the dependence of the transition dipoles on the charge number. In the following, we will only consider pumping of the neutral molecule and omit the q = 0 superscript on the transition dipoles. Throughout, we work in the interaction picture with respect to $H_{\rm int}(t) = H_{\rm v}(t) + H_{\rm x}(t)$ and in atomic units so that $\hbar = m_e = e = 1$. A straightforward application of the Fermi

Faraday Discussions Accepted Manuscript

View Article Online
DOI: 10.1039/C4FD00178H

Golden Rule gives the probability of generating a photoelectron in state $|\mathbf{p}\rangle$ to second order in the interaction with the ionizing pulse yields

$$P(\mathbf{p},T) = \sum_{II'} |E_{\mathrm{x}}\mu_{\mathbf{p}I'I}|^2 \delta(\omega_x - \varepsilon_{\mathbf{p}} - \mathcal{E}_{I_1'}(T) + \mathcal{E}_{I_0}(T))\rho_{I_0}(T), \tag{6}$$

where

$$\rho_{I_0}(T) \propto |E_{\mathrm{v}}\mu_{Ig}|^2 \delta(\omega_v - \mathcal{E}_{I_0}(0)) \tag{7}$$

is the population of state $|I_0\rangle$ and we have taken the snapshot limit of the pump and probe pulses (whereby the spectral and temporal pulse envelopes are both δ-functions with $\omega_{\mathrm{x}}, \omega_{\mathrm{v}}$ the frequency of the X-ray and valence pump pulses) and the signal is a function of the relative delay time T. The bound state energies (denoted with $\mathcal{E}$) and populations are still operators in the nuclear subspace and this expression must still be averaged over the nucelar degrees of freedom. This can be done formally with a model for the nucelar-electronic coupling or semiclassically by averaging over stochastic trajectories. This approach has the advantage of being very intuitive and is readily amenable to semiclassical treatments. Similar formulas have been used to study the nuclear dynamics on the excited singlet state potential energy surfaces of a variety of molecules [14, 15].

This expression however, makes several assumptions that may not apply for ultrafast experiments. One goal of this paper will be to elucidate these assumptions and how they may be relaxed to gain a better understanding of ultrafast dynamics.

III. LIOUVILLE SPACE DESCRIPTION OF TRPES

We define the signal as the integrated, energy-resolved photoelectron current:

$$S_{PES} = \int \frac{d}{dt}\langle n_{\mathbf{p}}(t)\rangle \tag{8}$$

Assuming that $[n_{\mathbf{p}}, H_{\mathrm{M}}] = 0$ (where $n_{\mathbf{p}} = c_{\mathbf{p}}^{\dagger}c_{\mathbf{p}}$ is the occupation number of the scattering state $|\mathbf{p}\rangle$), we have, from the Heisenberg equation of motion

$$\dot{n}_{\mathbf{p}} = -i[n_{\mathbf{p}}, H] = -2E_X(t)\Im\{\mu_{\mathbf{p}}\} \tag{9}$$

where

$$\mu_{\mathbf{p}} \equiv \sum_{I_0 I_1} \mu^*_{\mathbf{p}I_1I_0} c_{\mathbf{p}} |I_0\rangle\langle I_1| \tag{10}$$

The Liouville-Space treatment can rigorously incorporate "bath" degrees of freedom without explicitly treating them quantum mechanically. We treat the dynamics with the stochastic Liouville equation (SLE). It assumes that the quantum system of interest is affected by a classical bath, whose stochastic dynamics follows a Markovian master equation. The SLE is an equation of motion for the field-free evolution of the joint system density matrix:

$$|\dot{\rho}(t)\rangle\rangle = \mathcal{L}|\rho(t)\rangle\rangle = -iH_-|\rho(t)\rangle\rangle + L_b|\rho(t)\rangle\rangle \tag{11}$$

where H_- is the Liouville superoperator corresponding to commutation with the electronic Hamiltonian (see Appendix) and L_b represents the stochastic Markovian dynamics of the bath. The versatility of this approach lies both in the choice of which degrees of freedom are explicitly incoprorated into the Hamiltonian dynamics versus which are relegated to the bath and at what level the bath dynamics is treated (commonly, at least some of the nuclear degrees of freedom are treated as a semiclassical bath and solvent effects can be treated in this manner as well).

We describe a process in which a pump pulse populates the valence excited states, which then evolve for a delay period T before interaction with the x-ray probe. Assuming that the photoelectron state is initially vacant, the lowest order non-vanishing response has two interactions with the ionizing pulse. Since we are considering photoionization of an electronic excited state, we also expand to second order in the pump pulse. The Liouville-space signal can be read from the diagram in fig. (1):

$$S_{PES} = -2\int dt_4 dt_3 dt_2 dt_1 E_X(t_4)\Im\left[(i)^3\langle\langle \mathbb{1}|\mu_{\mathbf{p}L}(t_4)G(t_4,t_3)\mathcal{L}_{\mathrm{x}}(t_3)G(t_3,t_2)\mathcal{L}_{\mathrm{v}}(t_2)G(t_2,t_1)\mathcal{L}_{\mathrm{v}}(t_1)|gg\rangle\rangle\right] \tag{12}$$

Published on 04 November 2014. Downloaded by University of California - Irvine on 04/11/2014 18:23:19.
Faraday Discussions Accepted Manuscript

View Article Online
DOI: 10.1039/C4FD00178H

Published on 04 November 2014. Downloaded by University of California - Irvine on 04/11/2014 18:23:19.

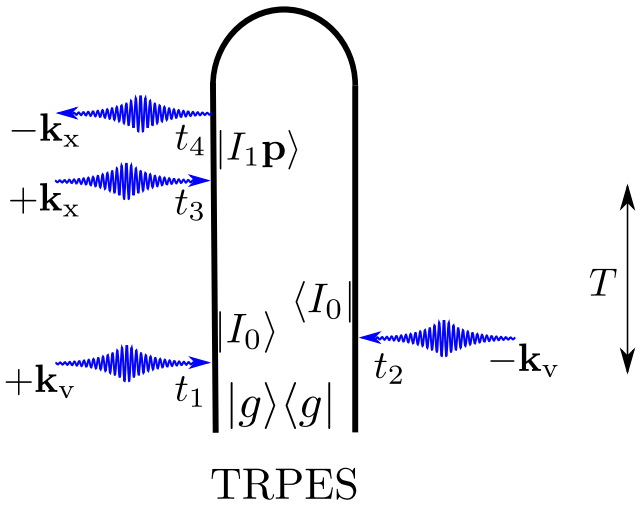

FIG. 1. Loop diagram for the TRPES process. The valence of both ket and bra are initially excited via an external pulse ($\mathbf{k}_v$). Following a delay T, the system interacts with an x-ray pulse ($\mathbf{k}_x$) which promotes an electron to the photoelectron continuum states ($\mathbf{p}$). This one loop diagram stands for two ladder diagrams since the valence pumping can occur first on the ket or first on the bra.

where

$$G(t,t') \equiv \theta(t-t')\exp[-i\mathcal{L}(t-t')] \tag{13}$$

is the Liouville space propagator and the L subscript indicates action on the ket (see Appendix). The initial density matrix is given by the pure state $|gg\rangle\rangle$ which corresponds to the many body ground state in which the core is full, the continuum is empty, and the valence states are occupied up to the some level. In principle all time propagations are with respect to H. However, assuming H conserves the charge number, we may write $H_{\rm M} = H_{\rm M}(\rm q)$ (as above, we assume $[n_{\mathbf{p}}, H] = 0$) . We then use projection operators to simplify the Green's functions in eq. (12). We work with the product states $|I_{\rm q}\rangle|\mathbf{p}\rangle \equiv |I_{\rm q}\mathbf{p}\rangle$ and the associated Liouville-space projection operators

$$\begin{aligned}
\mathcal{P}_1 &= \sum_{I_0} |I_0, g\rangle\rangle\langle\langle I_0, g| + |g, I_0\rangle\rangle\langle\langle g, I_0| \\
\mathcal{P}_2 &= \sum_{I_0} |I_0, I_0\rangle\rangle\langle\langle I_0, I_0| \\
\mathcal{P}_3 &= \sum_{I_0 I_1 \mathbf{p}} |I_1\mathbf{p}, I_0\rangle\rangle\langle\langle I_1\mathbf{p}, I_0|
\end{aligned} \tag{14}$$

which serve to restrict attention to particular manifolds of states. In particular, $\mathcal{P}_1$ projects into the space of coherences between the ground state and the $|0\rangle$ manifold (the set of states with 0 holes) and $\mathcal{P}_2$ projects into the space of populations of the $|0\rangle$ manifold and $\mathcal{P}_3$ projects into the space of coherences between the $|1\rangle$ and $|0\rangle$ manifolds (analogously to $\mathcal{P}_1$, $\mathcal{P}_3$ actually has two terms but we have kept only the one that contributes). Aside from the restriction to populations in $\mathcal{P}_2$ (this is justified for pulses separated by times larger than coherence decay times and is easily relaxed to account for overlapping pulses), inserting these projection operators entails no loss of generality since the Hamiltonian conserves the number of $\mathbf{p}$-electrons and holes. This is then equivalent to simply taking matrix elements by inserting resolutions of the identity operator. However, the use of projection operators makes clear how to include more complicated processes such as Auger decay which gives width to TRPES lines. We thus re-write the signal as

$$S_{PES} = -2\int dt_4 dt_3 dt_2 dt_1 E_X(t_4)\Im\left[(i)^3\langle\langle \mathbb{1}|\mu_{\mathbf{p}L}(t_4)G^{(3)}(t_4,t_3)\mathcal{L}_{\rm x}(t_3)G^{(2)}(t_3,t_2)\mathcal{L}_{\rm v}(t_2)G^{(1)}(t_2,t_1)\mathcal{L}_{\rm v}(t_1)|gg\rangle\rangle\right] \tag{15}$$

where

$$G^{(i)}(t,t') \equiv \mathcal{P}_i G(t,t')\mathcal{P}_i \tag{16}$$

Faraday Discussions Accepted Manuscript

View Article Online
DOI: 10.1039/C4FD00178H

Published on 04 November 2014. Downloaded by University of California - Irvine on 04/11/2014 18:23:19.

Inserting the definitions and expanding in eigenstates, we obtain

$$S_{PES} = -2\int dt_4 dt_3 dt_2 dt_1 \Im\Big[(i)^3 E_X^*(t_4)E_X(t_3)\sum_{II'}|\mu_{Ig}\mu_{\mathbf{p}I'I}|^2 G^{(3)}_{I_1'\mathbf{p},I_0}(t_4,t_3) \\ G^{(2)}_{I_0,I_0}(t_3,t_2)\{E^*_{UV}(t_2)E_{UV}(t_1)G^{(1)}_{I_0,g}(t_2,t_1) + E_{UV}(t_2)E^*_{UV}(t_1)G^{(1)}_{g,I_0}(t_2,t_1)\}\Big] \tag{17}$$

where we have made the rotating wave approximation (requiring that field excitation goes with material de-excitation and vice versa), and defined the shorthand:

$$G^{(i)}_{n,m}(t,t') \equiv G^{(i)}_{n'm',nm}(t,t')\delta_{n'n}\delta_{m'm} = \langle\langle n,m|G^{(i)}(t,t')|n,m\rangle\rangle \tag{18}$$

valid when $H_{I'I} = 0$. Non-adiabatic effects (which are frequently the objects of study in TRPES experiments) can cause electronic transitions and their inclusion therefore requires the full tetradic structure of the Green's functions. Since, in obtaining the semiclassical FGR result from the Liouville-space treatment, these considerations are only relevant for the middle propagation period $G^{(2)}(t_3,t_2)$, we ignore this complication on this first appraoch. To discuss the snapshot limit of pump-probe signals, it is convenient to utilize the Wigner spectrogram for the incoming pulses

$$E_i^*(t)E_i(t') = \int\frac{d\omega}{2\pi}\mathcal{W}_i\left(\frac{t+t'}{2},\omega\right)e^{i\omega(t-t')} \qquad i\in\{\mathrm{x},\mathrm{v}\} \tag{19}$$

and make the approximation of ideal time and frequency resolution

$$\mathcal{W}_i(t,\omega) = |E_i|^2\delta(t-t_i)\delta(\omega-\omega_i) \tag{20}$$

Since the field-free Hamiltonian is time-independent, we Fourier transform with respect to the difference times $\tau_i \equiv t_{i+1} - t_i$ giving

$$S_{PES}(T) = \frac{-2}{(2\pi)^2}|E_\mathrm{x}|^2|E_\mathrm{v}|^2\Im\Big[i\sum_{II'}|\mu_{Ig}\mu_{\mathbf{p}I'I}|^2 G^{(3)}_{I_1'\mathbf{p},I_0}(\omega_\mathrm{x})G^{(2)}_{I_0,I_0}(T)\{G^{(1)}_{I_0,g}(\omega_\mathrm{v}) + G^{(1)}_{g,I_0}(-\omega_\mathrm{v})\}\Big] \tag{21}$$

where we have defined $T = t_\mathrm{x} - t_\mathrm{v}$ and assumed that $G^{(2)}_{I_0,I_0}(T - \frac{\tau_1+\tau_3}{2}) \approx G^{(2)}_{I_0,I_0}(T)$ since $T \gg \tau_1,\tau_3$. Following [7], the coherence Green's function is

$$G_{n,m}(t) = \theta(t)e^{-iH_{nL}t}e^{iH_{mR}t} \tag{22}$$

and use the result that

$$G_{n,m}(t) = G_{m,m}(t)\mathrm{exp}_+^{-i\int_0^t d\tau U_L(\tau)} \tag{23}$$

where

$$U(t) \equiv e^{iH_m(t)}\left(H_n - H_m\right)e^{-iH_m(t)} \tag{24}$$

and $\exp_+$ is the positive time-ordered exponential. Equation (22) includes all degrees of freedom at the Hamiltonian level (and thus does not include bath degrees of freedom in the Liouvillian sense). This facilitates the semiclassical simulation of the nuclear dynamics and avoids the complication of solvent degrees of freedom (which are readily included in the form of an L_b operator). Recall that all parameters are functions of the time-dependent nuclear coordinates $\{\mathbf{q}\}(t)$ and so the signal given in eq. 21 must be averaged over the nuclear space. In the static (classical) limit, we neglect nuclear motions when the system is in an electronic coherence and $U(\tau)$ becomes time-independent

$$G_{n,m}(t) \approx e^{-iU_L t} \tag{25}$$

Note that this is an operator only in the nuclear subspace and so, under semiclassical approximation, is the ordinary exponential. In this limit, we have for the TRPES signal

$$S_{PES}(\varepsilon_\mathbf{p},T) = \sum_{I_1I_0}|E_\mathrm{x}\mu_{\mathbf{p}I_1I_0}|^2\delta(\omega_\mathrm{x} - \mathcal{E}_{I_1}(\{\mathbf{q}\}(T)) + \mathcal{E}_{I_0}(\{\mathbf{q}\}(T)) - \varepsilon_\mathbf{p})\rho_{I_0}(T) \tag{26}$$

Faraday Discussions Accepted Manuscript

View Article Online
DOI: 10.1039/C4FD00178H

where we have explicitly notated that the time dependence is through the set of nuclear coordinates $\{\mathbf{q}\}$ and

$$\rho_{I_0}(T) \equiv \sum_{I_0'} |E_{\rm v}\mu_{I_0'g}|^2 \delta(\omega_{\rm v} - \mathcal{E}_{I_0'}(\{\mathbf{q}\}(0))) G^{(2)}_{I_0 I_0, I_0' I_0'}(T) \tag{27}$$

is the population of the Ith state of $H(0)$ at time T including the effects of vibronic coupling. Neglecting these effects amounts to the substition $G^{(2)}_{I_0 I_0, I_0' I_0'}(T) = G^{(2)}_{I_0, I_0}(T)\delta_{I_0, I_0'}$. This represents the classical limit of the TRPES current. For practical simulations, the quantity $G^{(2)}_{I_0 I_0, I_0' I_0'}(T)$ is taken to be the population of the state initially excited to I_0' and propagated along a trajectory for a time T (I_0 is the final state to which the system is propagated) and is averaged over trajectories.

The finite widths of the pump and probe pulses can be included after the fact by convoluting with the field envelopes. This amounts to smearing the interaction time but keeps the bra and ket interaction times the same and amounts to neglecting electronic coherences. In cases where there is appreciable nuclear motion on ultrafast timescales (when the system is still in an electronic coherence), it will be necessary to go beyond this approximation and treat the coherence Green's function more exactly. Clearly, eq. (17) provides the most direct way to go beyond the static (classical) limit.

We take the field amplitudes to be the product of an envelope and a carrier frequency

$$E_i(t) = \tilde{E}_i(t - t_i)e^{-i\Omega_i(t-t_i)} + \text{c.c.} \qquad\qquad i \in \{\text{x}, \text{v}\} \tag{28}$$

where Ω_i is the carrier frequency for the pulse and $\tilde{E}_i(t)$ is the envelope (centered at $t = 0$). The time between the centers of the pulses is then $T = t_{\rm x} - t_{\rm v}$. To go beyond the static approximation, we allow for coupling between electronic levels, leaving the Green's function no longer diagonal.

$$S_{PES}(\varepsilon_{\mathbf{p}}, T) = \Im\Big[\sum_{\{I_0, I_1\}} \int_0^\infty d\tau_3 \int_0^\infty d\tau_2 \int_0^\infty d\tau_1 \mu^*_{\mathbf{p}I_1' I_0'''} \mu_{\mathbf{p}I_1 I_0''} G^{(3)}_{I_1'\mathbf{p}I_0''', I_1\mathbf{p}I_0''}(\tau_3) G^{(2)}_{I_0''I_0'', I_0'I_0'}(\tau_2) \tag{29}$$

$$\times \{\mu_{gI_0'}\mu_{I_0 g} G^{(1)}_{I_0'g, I_0 g}(\tau_1) + \mu_{gI_0}\mu_{I_0' g} G^{(1)}_{gI_0', gI_0}(\tau_1)\} \int dt_4 \tilde{E}_{\rm x}(t_4)\tilde{E}_{\rm x}(t_4 - \tau_3)\tilde{E}_{\rm v}(t_4 - \tau_3 - \tau_2)\tilde{E}_{\rm v}(t_4 - \tau_3 - \tau_2 - \tau_1)\Big]$$

where $\sum_{\{I_0, I_1\}}$ indicates summation over the set of state indices. As a first approximation to the extensions to the FGR expression, we treat the electronic gap coordinate as a function rather than an operator (treating the nuclear coordinates semiclassically) so that the time-ordered exponential reduces to a standard exponential. We then utilize eq. (23) to express the coherence Green's functions in terms of population Greens functions which have direct classical analogs. This results in

$$S_{PES}(\varepsilon_{\mathbf{p}}, T) = \Im\Big[\sum_{\{I_0, I_1\}} \int_0^\infty d\tau_3 \int_0^\infty d\tau_2 \int_0^\infty d\tau_1 \mu^*_{\mathbf{p}I_1' I_0'''} \mu_{\mathbf{p}I_1 I_0''} \{\mu_{gI_0'}\mu_{I_0 g} e^{i(-\bar{U}_1 + \Omega_{\rm v})\tau_1} + \mu_{gI_0}\mu_{I_0' g} e^{i(\bar{U}_1 - \Omega_{\rm v})\tau_1}\} e^{i(\bar{U}_3 + \Omega_{\rm x} - \varepsilon_{\mathbf{p}})\tau_3} \tag{30}$$

$$\times G^{(2)}_{I_0'''I_0''', I_0''I_0''}(\tau_3) G^{(2)}_{I_0''I_0'', I_0'I_0'}(\tau_2) G^{(2)}_{I_0'I_0', I_0 I_0}(\tau_1) \int dt_4 \tilde{E}_{\rm x}(t_4)\tilde{E}_{\rm x}(t_4 - \tau_3)\tilde{E}_{\rm v}(t_4 - \tau_3 - \tau_2)\tilde{E}_{\rm v}(t_4 - \tau_3 - \tau_2 - \tau_1)\Big]$$

where the auxilliary quantities

$$\bar{U}_1 \equiv \frac{1}{\tau_1}\int_0^{\tau_1} d\tau' \mathcal{E}_{I_0 \to I_0'}(\tau') - \mathcal{E}_g(\tau') \qquad\qquad \bar{U}_3 \equiv \frac{1}{\tau_3}\int_0^{\tau_3} d\tau' \mathcal{E}_{I_1 \to I_1'}(\tau') - \mathcal{E}_{I_0'' \to I_0'''}(\tau') \tag{31}$$

are the time-averaged electronic gap coordinates for time periods τ_1 and τ_3 where the time averaging is done for each trajectory (symbolized by the $\mathcal{E}_{i\to f}$). As a reminder, we have assumed the Franck-Condon approximation without which the transition dipoles would depend parametrically on time through their dependence on the nuclear coordinates. All Green's functions remain operators in the nuclear subspace and so eqs. (26) and (30) must be averaged over these degrees of freedom (although this is not explicitly notated in the above).

For cases in which environmental and vibronic couplings between excited states are particularly simple, it is frequently more convenient to treat the problem in Hilbert space. We therefore give the TRPES signal in this form as well for completeness.

$$S_{PES}(\varepsilon_{\mathbf{p}}, T) = \Im\Big[\sum_{\{I_0, I_1\}} \int dt_4 dt_3 dt_3 dt_1 \tilde{E}_{\rm x}(t_4)\tilde{E}_{\rm x}(t_3)\tilde{E}_{\rm v}(t_2)\tilde{E}_{\rm v}(t_1) \tag{32}$$

$$\langle \mu_{gI_0'}(t_2)\mathcal{G}^-_{I_0', I_0'''}(t_2, t_4)\mu^*_{\mathbf{p}I_1' I_0'''}(t_4)\mathcal{G}^+_{I_1'\mathbf{p}, I_1\mathbf{p}}(t_4, t_3)\mu_{\mathbf{p}I_1 I_0''}(t_3)\mathcal{G}^+_{I_0'', I_0}(t_3, t_1)\mu_{I_0 g}(t_1)\rangle\Big]$$

Published on 04 November 2014. Downloaded by University of California - Irvine on 04/11/2014 18:23:19.

Faraday Discussions Accepted Manuscript

View Article Online
DOI: 10.1039/C4FD00178H

TABLE I. Calculated excitation energies at the Franck-Condon point in eV. The Experimental value is taken from ref. [37]

.

transition	calc.	exp.
$S_0 \to S_1$ $(n \to \pi^*)$	3.6279	
$S_0 \to S_2$ $(n \to \pi^*)$	6.8740	
$S_0 \to S_3$ $(\pi \to \pi^*)$	7.5165	6.41(193 nm)

where

$$\mathcal{G}^+_{ij}(t,t') = \theta(t-t')\langle i|\exp_+^{-i\int_t^{t'} H(\tau)d\tau}|j\rangle \qquad \mathcal{G}^-_{ij}(t,t') = \theta(t'-t)\langle i|\exp_-^{i\int_t^{t'} H(\tau)d\tau}|j\rangle \tag{33}$$

are the Hilbert space forward and backward propagators ($\exp_-$ is the negative time-ordered exponential) and we have explicitly notated the time dependence of the transition dipole moments (which is only relevent outside the Franck-Condon approximation) and the averaging over the nuclear subspace (represented by $\langle \dots \rangle$).

IV. CONICAL INTERSECTIONS IN TRANS-ACROLEIN

We present the simulation for a valence TRPES of trans-acrolein (propenal). The molecule has a conjugated π-system composed from the C=C double bond and the carbonyl group (C=O) making it an ideal system to investigate the non-adiabatic excited state dynamics. The quantum chemistry calculations are carried out with MOLPRO [36] at the complete active space self consistent field (CASSCF) level of theory (sa4-CAS(6/5)/6-31+G*) with 6 electrons in 5 active orbitals. The molecular orbitals (MOs) occupied in the electronic ground state are two π-orbitals for the CC and the CO bond as well as the oxygen lone pair. The lowest unoccupied molecular orbitals (LUMOs) correspond to the first two π^*-orbitals. It turns out that, a the given level of theory, 4 states have to be taken in account. The S_2 and S_3 state are separated by $\approx$0.65 eV at the Franck-Condon point. Moreover, the S_2 and S_3 state are coupled by a conical intersection which is in reach within the first 25 fs of the time evolution. The excitation energies calculated at CAS level are given in tab. I. A vertical, resonant UV excitation is most favorable for the $S_0 \to S_3$ transition with a transition dipole moment of 0.18 au as opposed to the $S_0 \to S_2$ transition, which is much weaker ($\mu_{S2,S0}$=0.044 au).

The nuclear dynamics triggered by the UV excitation is calculated by the Tully surface hopping (SH) algorithm [38] (NEWTON-X [39] with a home made interface to MOLPRO). Here, the dynamics of the nuclei is described by the classical equations of motion, while the electronic degrees of freedom are treated quantum mechanically (sa4-CAS(5/6)/6-31+G*). The forces acting on the nuclei are derived from the gradient of a particular electronic state the trajectory is in at time T. We interpret the population ρ_{I_0,I_0} of an electronic state I_0 as the average over all N trajectories:

$$\rho_{I_0,I_0}(t) = \frac{1}{N}\sum_{i=1}^{N} \delta_{s_i(t),I_0}\,, \tag{34}$$

where $s_i(t)$ is the electronic state of trajectory i. The initial state populated by the UV pulse is the electronic S_3 state. We make the simplifying assumption that the excitation is sudden, thereby neglecting possible Franck-Condon factors. All states are coupled to each other by conical intersections (CoIns) and consecutive state jumps back to the ground state are observed in our trajectory simulations as well as under experimental conditions [37]. The time evolution of ρ_{I_0,I_0} is shown in fig. 2 for the first 500 fs. The S_3 state undergoes a rapid decay via a close by non-adiabatic coupling to the S_2 state transferring half of its population into the S_2 state. The S_1 state is populated in a next step and reaches about 40% within 250 fs.

The TRPES spectra, we use the semiclassical (FGR) expression obtained in eq. (26). The population Greens-function from eq. (27) is realized by the SH algorithm on the excited neutral states. In the SH method the electronic state populations are obtained by averaging over a large number of trajectories. The TRPES signal S_{PES} is then given by the sum over all N trajectories:

$$S_{PES,SH} = \sum_{n=1}^{N}\sum_{I_1} |E_{\mathrm{x}}\mu_{\mathbf{p}I_1I_0}|^2\delta(\omega_{\mathrm{x}} - \mathcal{E}_{I_1}(T) + \mathcal{E}_{I_0}(T) - \varepsilon_{\mathbf{p}})\rho_{I_0,n}(T) \tag{35}$$

Note that the final state of the propagation (I_0) is not summed over since this averaging process is accounted for in the trajectory summation. Every trajectory is in a specific state I_0 at time T. Moreover it is assumed that the UV

Published on 04 November 2014. Downloaded by University of California - Irvine on 04/11/2014 18:23:19.
Faraday Discussions Accepted Manuscript

View Article Online
DOI: 10.1039/C4FD00178H

Published on 04 November 2014. Downloaded by University of California - Irvine on 04/11/2014 18:23:19.

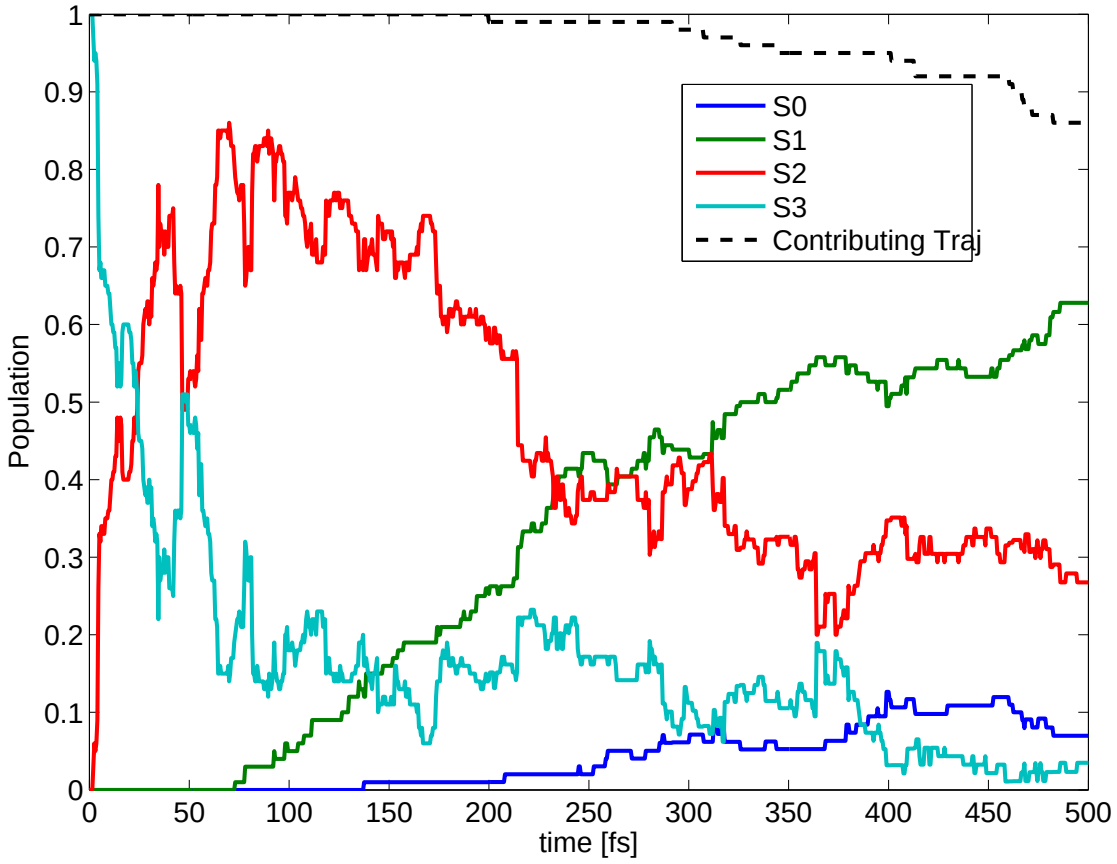

FIG. 2. Population of the electronic states vs. time. The total number of contributing trajectories is 100 generated from a Wigner distribution at 0 K. The Initial state is the S_3 state.

excitation pulse is resonant with a specific electronic state (I_0') at $T = 0$ to yield the initial condition (state) for all trajectories.

$$\rho_{I_0,n}(T) \equiv |E_{\mathrm{v}}\mu_{I_0 g}|^2 G^{(2)}_{I_0 I_0, I_0' I_0'}(T) \tag{36}$$

The x-ray ionization pulse is given a finite width in frequency by replacing the δ in function in eq. 35 by a Gaussian giving the final expression:

$$S_{PES,SH} \approx \sum_{n=1}^{N} \sum_{I_1} |E_{\mathrm{x}}\mu_{\mathbf{p}I_1 I_0}|^2 e^{-\left(\omega_{\mathrm{x}} - \mathcal{E}_{I_1}(T) + \mathcal{E}_{I_0}(T) - \varepsilon_{\vec{p}}\right)^2 / 2\sigma_\omega^2} \rho_{I_0,n}(T) \tag{37}$$

To incorporate the ionized states into the simulations the corresponding ionic doublet states D_0 - D_4 are calculated at a similar level of theory (sa5-CAS(5/5)/6-31+G*) as the neutral states. The different size of the active space and the fact that CASSCF is not a size consistent introduces a small but negligible systematic error. The transition dipole moments $\mu_{\mathbf{p}I_1 I_0}$ from the neutral to ionic states is approximated by utilizing Dyson orbitals [14, 40, 41]:

$$\Phi^D_{I_0,I_1}(\vec{r}) = \sqrt{N} \int d\vec{r}_1 ... d\vec{r}_{N-1} \Psi_{I_0}(\vec{r}_1 ... \vec{r}_N) \Psi_{I_1}(\vec{r}_1 ... \vec{r}_{N-1}) \tag{38}$$

where Ψ_{I_0} is the electronic wave function of the neutral molecule and Ψ_{I_1} the ion wave function for a particular snapshot. The norm of the Dyson orbital $\langle \Phi^D_{I_0,I_1} | \Phi^D_{I_0,I_1} \rangle$ is proportional to the ionization probability [14, 42]. In MO basis $\Phi^D_{I_0,I_1}$ can be written as:

$$\Phi^D_{I_0,I_1}(\vec{r}) = \sum_{\alpha} \phi_\alpha(\vec{r}) \langle \Psi_{I_1} | a_\alpha | \Psi_{I_0} \rangle \tag{39}$$

Faraday Discussions Accepted Manuscript

View Article Online
DOI: 10.1039/C4FD00178H

Here a_α is an annihilation operator which removes an electron from the MO ϕ_α. In the case of a CASSCF wave function the index α runs over all orbitals in the active space and Φ^D can be expanded in the Slater determinants $\psi_{I_0,i}$ and $\psi_{I_1,j}$ and their corresponding configuration interaction (CI) coefficients $c_{I_0,i}$ and $c_{I_1,j}$ [14]:

$$\Phi^D_{I_0,I_1}(\vec{r}) = \sum_\alpha \phi_\alpha(\vec{r}) \sum_{i,j} c_{I_0,i} c_{I_1,j} \langle \psi_{I_1,j} | a_\alpha | \psi_{I_0,i} \rangle \tag{40}$$

The overlap factor in eq. (40) between the different configurations is determined by calculating the overlap between the slater determinants of the ionic and neutral states:

$$\langle \psi_{I_1,j} | a_\alpha | \psi_{I_0,i} \rangle = \langle \phi'_1 ... \phi'_{\alpha-1} \phi'_{\alpha+1} ... \phi'_N | \phi_1 ... \phi_{\alpha-1} \phi_{\alpha+1} ... \phi_N \rangle = \det(\langle \phi'_n | \phi_m \rangle) \tag{41}$$

where ϕ'_n and ϕ_m are the MOs of the ionic and neutral wave function respectively. The MOs of neutral state form orthonormal set and the norm of the Dyson orbitals, giving the weight factor for the ionization probability, can be written as:

$$\langle \Phi^D_{I_0,I_1} | \Phi^D_{I_0,I_1} \rangle = \sum_\alpha |\langle \Psi_{I_1} | a_\alpha | \Psi_{I_0} \rangle|^2 . \tag{42}$$

By using the norm of the Dyson orbitals a possible dependence of the transition dipole moment on the photo electron kinetic energy is neglected as well as any directional dependence. Combining eqs. (37) and (42) the approximated photo electron signal can then be written as:

$$S_{PES,SH} \approx \sum_{n=1}^{N} \sum_{I_1} |E_\mathrm{x}|^2 \langle \Phi^D_{I_0,I_1} | \Phi^D_{I_0,I_1} \rangle e^{-\left(\omega_\mathrm{x} - \mathcal{E}_{I_1}(T) + \mathcal{E}_{I_0}(T) - \varepsilon_{\vec{p}}\right)^2 / 2\sigma_\omega^2} \rho_{I_0,n}(T) \tag{43}$$

The photoelectron spectrum calculated with eq. (43) is shown in fig. 3. The photon energy of the pulse is chosen to be 12 eV (103 nm) with a FWHM of 0.71 eV which corresponds to 5 fs temporal width. The shape of the spectrum reproduces the main features of the trajectory calculations as shown in fig. 2. This is the fast decay to the S_2 state within the first 25 fs after the UV excitation and the increase in population in S_1 between 150 and 250 fs. The population in S_1 can attributed to the band around 2 eV, while the S_2 state population is visible through the band around 4.5 eV. Over the whole time evolution the variation due to nuclear motion is clearly visible in the TRPES. From these fast features the improvements to the TRPES model introduced in the previous sections can be directly motivated. If excitation and ionization pulses with lengths of several femtoseconds length are used then a description beyond the semi classical limit can provide a substantial improvement. A direct propagation approach for the fast molecular vibrations (e.g. C-H stretch vibrations) which treats them by a full quantum model even opens up the route for coupling TRPES with vibrational spectroscopy methods like FSRS.

V. TIME-RESOLVED AUGER SIGNALS

The above description of TRPES is suitable for photoionization of both valence and core electrons. However, a treatment of core TRPES should distinguish between core and valence holes. Obviously, this is necessary for a description of Auger decay and Auger-electron spectroscopy. For this reason, in this section, the q subscript on the molecular states will be reserved for core holes. States with two fewer valence electrons than the neutral molecule (dicationic valence states) will then be denoted by $\tilde{I}$.

In order to describe Auger decay of core holes generated via TRPES processes, we add the following terms to the Hamiltonian:

$$H_\mathbf{k} = \sum_\mathbf{k} \varepsilon_\mathbf{k} c^\dagger_\mathbf{k} c_\mathbf{k} \qquad\qquad A = \sum_{\mathbf{k}\tilde{I}I} A_{\mathbf{k}\tilde{I}I} c^\dagger_\mathbf{k} |\tilde{I}_0\rangle\langle I_1| + h.c. \tag{44}$$

where $H_\mathbf{k}$ is the Hamiltonian of the Auger electron continuum states (which, following [23], we take to be energetically well-separated from any photoelectron states so that their Hamiltonians commute) and the A-operator induces Auger transitions. For clarity, this is represented in a fully microscopic manner with a fermionic second-quantized description of the molecular states (core and valence levels) in the appendix. For the moment, we leave the expression in this more model-independent form. As for TRPES, the signal is defined as the integrated electron current

$$S_A = \int \frac{d}{dt} \langle n_\mathbf{k}(t) \rangle = -i[n_\mathbf{k}, H_T] = -2\Im\left[A_\mathbf{k}\right] \tag{45}$$

Published on 04 November 2014. Downloaded by University of California - Irvine on 04/11/2014 18:23:19.
Faraday Discussions Accepted Manuscript

View Article Online
DOI: 10.1039/C4FD00178H

Published on 04 November 2014. Downloaded by University of California - Irvine on 04/11/2014 18:23:19.

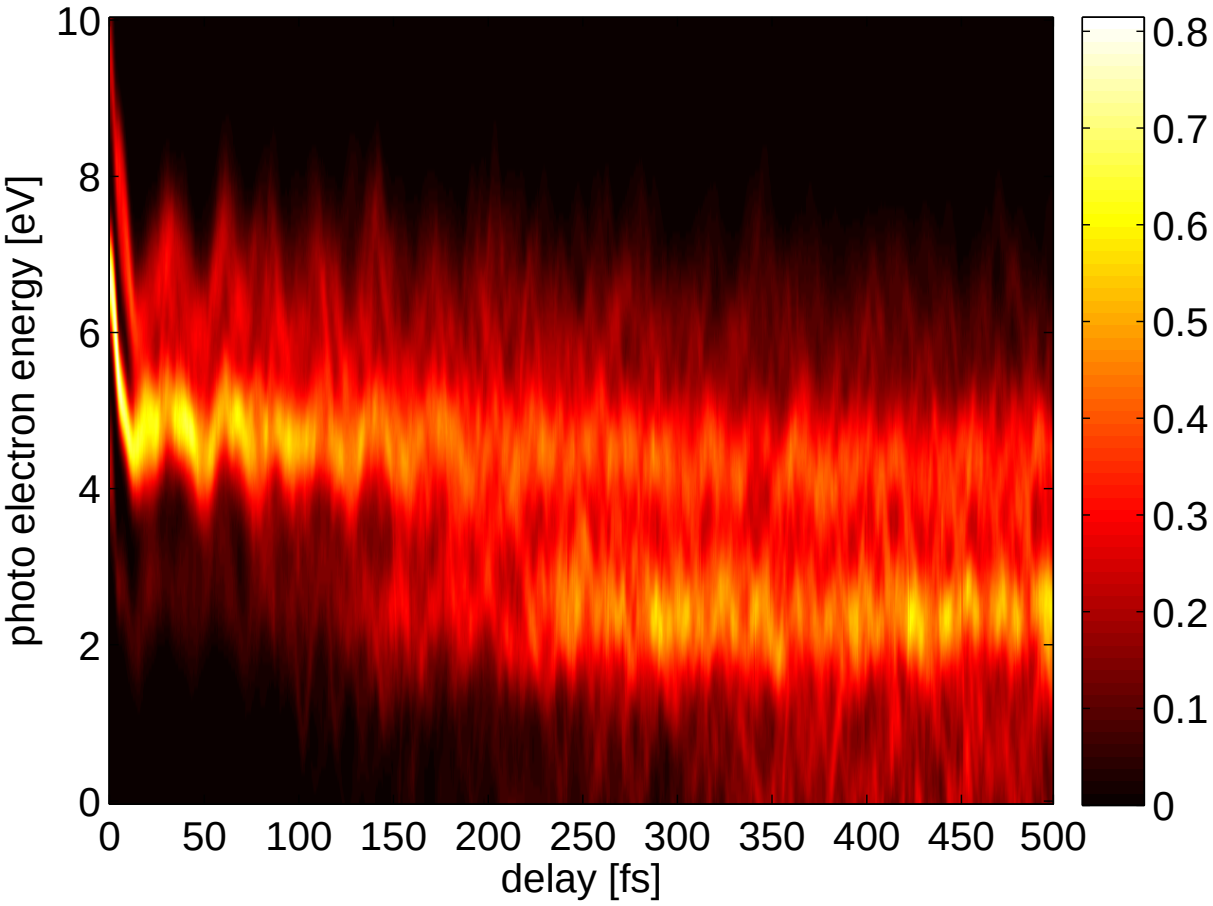

FIG. 3. TRPES for an ionization pulse with a photon energy of 12 eV and a FWHM of 5 fs. The intensity is given in arbitrary units.

where

$$A_{\mathbf{k}} \equiv \sum_{\tilde{I}I} A^{*}_{\mathbf{k}\tilde{I}I} c_{\mathbf{k}} |I_1\rangle\langle\tilde{I}_0|. \tag{46}$$

The Auger electrons originate from decay of the TRPES core hole and the description therefore contains more propagators compared to TRPES. Since the Auger states are initially unoccupied, the signal vanishes to zero order and must be expanded at least once in $A_{\mathbf{k}}$. Keeping only this term (which is second order in the Auger coupling) and expanding to second order in the interactions with the external pulses gives

$$S_A = -2 \int dt_6 \dots dt_1 \Im\Big[(i)^5 \langle\langle \mathbb{1}| A_{\mathbf{k}} G(t_6,t_5) A^{\dagger}_{\mathbf{k}} G(t_5,t_4) \mathcal{L}_{\mathrm{x}}(t_4) G(t_4,t_3) \mathcal{L}_{\mathrm{x}}(t_3) G(t_3,t_2) \mathcal{L}_{\mathrm{v}}(t_2) G(t_2,t_1) \mathcal{L}_{\mathrm{v}}(t_1) |gg\rangle\rangle\Big] \tag{47}$$

The inclusion of the Auger electron necessitates an additional state label

$$|\tilde{I}\rangle|\mathbf{p}\rangle|\mathbf{k}\rangle \equiv |\tilde{I}\mathbf{p}\mathbf{k}\rangle \tag{48}$$

As described above, when discussing core TRPES and Auger-electron spectroscopy, we use I_q to index states of the molecule that have q core holes and the same number of valence electrons as the neutral molecule. In Auger processes, we must also consider states of the dicationic valence (valence states with two fewer electrons than valence states of the neutral molecule). Such states will be labeled with a "tilde" $\tilde{I}_q$. In addition to the projection operators defined

Faraday Discussions Accepted Manuscript

View Article Online
DOI: 10.1039/C4FD00178H

Published on 04 November 2014. Downloaded by University of California - Irvine on 04/11/2014 18:23:19.

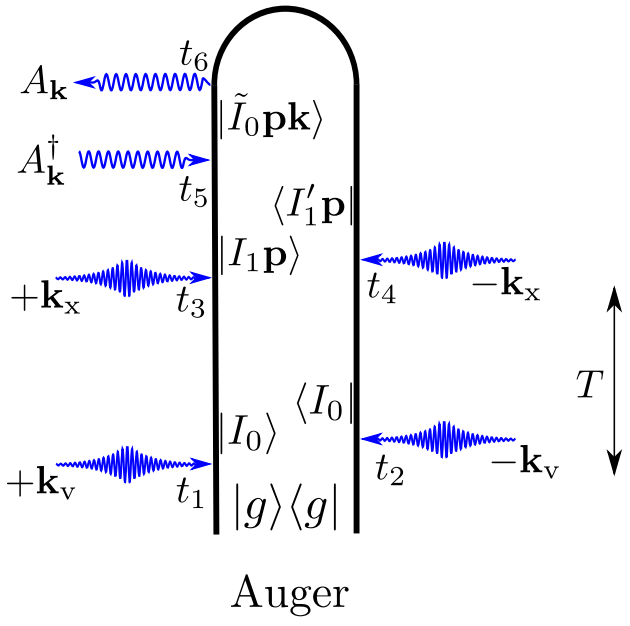

FIG. 4. Loop diagram for the Auger decay process. As before, the valence of both ket and bra are initially excited via an external pulse ($\mathbf{k}_\mathrm{v}$) and then photoionized via an X-ray pulse ($\mathbf{k}_\mathrm{x}$) following a delay time T. The system then evolves under the influence of the Hamiltonian including the Auger decay term and emits an Auger electron. This one loop diagram stands for 4 ladder diagram in Liouville space as each interaction with the external fields can be in either order (ket first and then bra or vice-versa).

previously, we introduce:

$$\mathcal{P}_3 = \sum_{I_0 I_1 \mathbf{p}} |I_1\mathbf{p}, I_0\rangle\rangle\langle\langle I_1\mathbf{p}, I_0| + |I_0 I_1\mathbf{p}\rangle\rangle\langle\langle I_0, I_1\mathbf{p}| \tag{49}$$
$$\mathcal{P}_4 = \sum_{I_1 I'_1 \mathbf{p}} |I_1\mathbf{p}, I'_1\mathbf{p}\rangle\rangle\langle\langle I_1\mathbf{p}, I'_1\mathbf{p}|$$
$$\mathcal{P}_5 = \sum_{I_1 \tilde{I}_0 \mathbf{p}\mathbf{k}} |\tilde{I}_0\mathbf{p}\mathbf{k}, I_1\mathbf{p}\rangle\rangle\langle\langle \tilde{I}_0\mathbf{p}\mathbf{k}, I_1\mathbf{p}|$$

With which the signal is then expressed as

$$S_A = -2\int dt_6 dt_5 dt_4 dt_3 dt_2 dt_1 \tag{50}$$
$$\Im\Big[(i)^5\langle\langle \mathbb{1}|A_{\mathbf{k}}G^{(5)}(t_6,t_5)A^\dagger_{\mathbf{k}}G^{(4)}(t_5,t_4)\mathcal{L}_\mathrm{x}(t_4)G^{(3)}(t_4,t_3)\mathcal{L}_\mathrm{x}(t_3)G^{(2)}(t_3,t_2)\mathcal{L}_\mathrm{v}(t_2)G^{(1)}(t_2,t_1)\mathcal{L}_\mathrm{v}(t_1)|gg\rangle\rangle\Big]$$

with the $G^{(i)}$ defined as before. Substituting the interaction Liouvillians and formally evaluating matrix elements gives

$$S_A = -2\int dt_6 dt_5 dt_4 dt_3 dt_2 dt_1 \Im\Big[(i)^5\int d\varepsilon_{\mathbf{p}} \sum_{I_0 I_1 I'_1 \tilde{I}_0} |\mu_{I_0 g}|^2 A_{\mathbf{k}\tilde{I}_0 I_1} A^*_{\mathbf{k}\tilde{I}_0 I'_1}\mu_{\mathbf{p}I_1 I_0}\mu *_{\mathbf{p}I'_1 I_0} G^{(5)}_{\tilde{I}_0\mathbf{p}\mathbf{k},I'_1\mathbf{p}}(t_6,t_5)G^{(4)}_{I_1\mathbf{p},I'_1\mathbf{p}}(t_5,t_4) \tag{51}$$
$$\{E^*_\mathrm{x}(t_4)E_\mathrm{x}(t_3)G^{(3)}_{I_1\mathbf{p},I_0}(t_4,t_3) + E^*_\mathrm{x}(t_4)E_\mathrm{x}(t_3)G^{(3)}_{I_0,I_1\mathbf{p}}(t_4,t_3)\}G^{(2)}_{I_0,I_0}(t_3,t_2)\{E^*_\mathrm{v}(t_2)E_\mathrm{v}(t_1)G^{(1)}_{I_0,g}(t_2,t_1) + E_\mathrm{v}(t_2)E^*_\mathrm{v}(t_1)G^{(1)}_{g,I_0}(t_2,t_1)\}\Big]$$

where we have taken the Green's functions to be diagonal for now. Changing to delay times and employing the

Faraday Discussions Accepted Manuscript

View Article Online
DOI: 10.1039/C4FD00178H

Published on 04 November 2014. Downloaded by University of California - Irvine on 04/11/2014 18:23:19.

snapshot limit of pulses as before, this becomes

$$S_A = -2\int dt_6 d\tau_5 |E_{\rm x}E_{\rm v}|^2 \Im\Big[(i)^3 \sum_{I_0 I_1 I_1' \tilde{I}_0 \mathbf{p}} |\mu_{I_0 g}|^2 A_{\mathbf{k}\tilde{I}_0 I_1} A^*_{\mathbf{k}\tilde{I}_0 I_1'} \mu_{\mathbf{p}I_1 I_0} \mu *_{\mathbf{p}I_1' I_0} G^{(5)}_{\tilde{I}_0\mathbf{p}\mathbf{k},I_1'\mathbf{p}}(\tau_5) \tag{52}$$

$$G^{(4)}_{I_1\mathbf{p},I_1'\mathbf{p}}(t_6 - t_x - \tau_5))\{G^{(3)}_{I_1\mathbf{p},I_0}(\omega_{\rm x}) + G^{(3)}_{I_0,I_1'\mathbf{p}}(-\omega_{\rm x})\}G^{(2)}_{I_0,I_0}(T)\{G^{(1)}_{I_0,g}(\omega_{\rm v}) + G^{(1)}_{g,I_0}(-\omega_{\rm v})\}\Big]$$

where we have Fourier transformed with respect to τ_1, τ_3 and have used the approximations $G^{(4)}_{I_1\mathbf{p},I_1'\mathbf{p}}(t_6 - t_x - \tau_5 - \tau_3/2) \approx G^{(4)}_{I_1\mathbf{p},I_1'\mathbf{p}}(t_6 - t_x - \tau_5)$ and $G^{(2)}_{I_0,I_0}(T - \frac{\tau_1+\tau_3}{2}) \approx G^{(2)}_{I_0,I_0}(T)$ justified in the limit of ultrashort, well-separated excitation and ionization pulses. Substituting $G^{(4)}$ with its Fourier Transform and carrying out the dt_6 integration gives

$$S_A(\mathbf{k},T) = -2|E_{\rm x}E_{\rm v}|^2 \Im\Big[i \sum_{I_0 I_1 I_1' \tilde{I}_0 \mathbf{p}} |\mu_{I_0 g}|^2 A_{\mathbf{k}\tilde{I}_0 I_1} A^*_{\mathbf{k}\tilde{I}_0 I_1'} \mu_{\mathbf{p}I_1 I_0} \mu *_{\mathbf{p}I_1' I_0} G^{(5)}_{\tilde{I}_0\mathbf{p}\mathbf{k},I_1'\mathbf{p}}(\omega=0) G^{(4)}_{I_1\mathbf{p},I_1'\mathbf{p}}(\omega=0) \tag{53}$$

$$\{G^{(3)}_{I_1\mathbf{p},I_0}(\omega_{\rm x}) + G^{(3)}_{I_0,I_1'\mathbf{p}}(-\omega_{\rm x})\}G^{(2)}_{I_0,I_0}(T)\{G^{(1)}_{I_0,g}(\omega_{\rm v}) + G^{(1)}_{g,I_0}(-\omega_{\rm v})\}\Big]$$

where we have written the arguments of $G^{(4)}$,$G^{(5)}$ so as to make clear that they are frequency-domain Green's functions. Since the ket and bra of $G^{(4)}_{I_1\mathbf{p},I_1'\mathbf{p}}$ are summed over the same manifold of states, its principal value vanishes and we make the substitution

$$G^{(4)}_{I_1\mathbf{p},I_1'\mathbf{p}}(\omega=0) = -i\pi\delta(\mathcal{E}_{I_1}(T) - \mathcal{E}_{I_1'}(T)) \tag{54}$$

which restricts the valence to be in a population during the τ_4 time period. Combining the Green's functions for the periods τ_1 and τ_3 yields

$$S_A(\mathbf{k},T) = 2|E_{\rm x}E_{\rm v}|^2 \int d\varepsilon_{\mathbf{p}} \sum_{I_0 I_1 I_1' \tilde{I}_0} |\mu_{I_0' g}\mu_{\mathbf{p}I'I} A_{\mathbf{k}\tilde{I}I}|^2 \delta(\varepsilon_{\mathbf{k}} + \mathcal{E}_{\tilde{I}_0}(T) - \mathcal{E}_{I_1}(T)) \tag{55}$$

$$\delta(\omega_{\rm x} + \mathcal{E}_{I_0}(T) - \mathcal{E}_{I_1}(T) - \varepsilon_{\mathbf{p}}) G^{(2)}_{I_0 I_0, I_0' I_0'}(T)\delta(\omega_{\rm v} - \mathcal{E}_{I_0}(0))$$

This is the semiclassical FGR result and is easily convoluted with spectral pulse envelopes, detector sensitivity functions, etc. to simulate the Auger spectra. As with TRPES, we have made several assumptions in arriving at this simplified expression. Principally, this takes the nuclei as frozen during electronic coherences. Although this is well-justified in the limit of ultrafast, well-separated pulses, it is certainly open to question in the case of excitation by overlapping or broader pulses during which processes the system may spend non-trivial amounts of time in electronic coherence. Equation (51) provides an ideal starting point for going beyond this semi-classical limit.

$$S_A(\varepsilon_{\mathbf{k}},T) = 2\Im\Big[i\int d\varepsilon_{\mathbf{p}} \sum_{\{I_0,I_1\tilde{I}_0\}} \int dt_6 \ldots dt_1 \tilde{E}_{\rm x}(t_4)\tilde{E}_{\rm x}(t_3)\tilde{E}_{\rm v}(t_2)\tilde{E}_{\rm v}(t_1) G^{(5)}_{\tilde{I}_0'\mathbf{k}\mathbf{p}I_1''\mathbf{p},\tilde{I}_0\mathbf{k}\mathbf{p}I_1'\mathbf{p}}(t_6,t_5) G^{(4)}_{I_1''\mathbf{p}I_1''\mathbf{p},I_1'\mathbf{p}I_1'\mathbf{p}}(t_5,t_4) \tag{56}$$

$$\times \{\mu^*_{\mathbf{p}I_1'I_0'''}\mu_{\mathbf{p}I_1I_0''} G^{(3)}_{I_1'\mathbf{p}I_0''',I_1\mathbf{p}I_0''}(t_4,t_3) + \mu^*_{\mathbf{p}I_1I_0''}\mu_{\mathbf{p}I_1'I_0''} G^{(3)}_{I_0'''I_1'\mathbf{p},I_0''I_1\mathbf{p}}(t_4,t_3)\}$$

$$\times G^{(2)}_{I_0''I_0'',I_0'I_0'}(t_3,t_2)\{\mu_{gI_0'}\mu_{I_0g} G^{(1)}_{I_0'g,I_0g}(t_2,t_1) + \mu_{gI_0}\mu_{I_0'g} G^{(1)}_{gI_0',gI_0}(t_2,t_1)\}\Big]$$

where, for brevity, we have retained the interaction times (t_i) in favor of the delay periods (τ_i). As before, we may rewrite this in terms of populations Green's functions and propagated phase factors representing the electronic energy gaps

$$S_A(\varepsilon_{\mathbf{k}},T) = 2\Im\Big[i\int d\varepsilon_{\mathbf{p}} \sum_{\{I_0,I_1\tilde{I}_0\}} \int dt_6 \ldots dt_1 \tilde{E}_{\rm x}(t_4)\tilde{E}_{\rm x}(t_3)\tilde{E}_{\rm v}(t_2)\tilde{E}_{\rm v}(t_1) e^{i(\bar{U}_5+\varepsilon_{\mathbf{k}})(t_6-t_5)} G^{(4)}_{I_1'''I_1''',I_1''I_1''}(t_6,t_5) \tag{57}$$

$$\times G^{(4)}_{I_1''I_1''',I_1'I_1'}(t_5,t_4)\{\mu^*_{\mathbf{p}I_1'I_0'''}\mu_{\mathbf{p}I_1I_0''} e^{i(\bar{U}_3+\Omega_{\rm x}-\varepsilon_{\mathbf{p}})(t_4-t_3)} + \mu^*_{\mathbf{p}I_1I_0''}\mu_{\mathbf{p}I_1'I_0''} e^{-i(\bar{U}_3+\Omega_{\rm x}-\varepsilon_{\mathbf{p}})(t_4-t_3)}\}$$

$$\times G^{(2)}_{I_0'''I_0''',I_0''I_0''}(t_4,t_3) G^{(2)}_{I_0''I_0'',I_0'I_0'}(t_3,t_2) G^{(2)}_{I_0'I_0',I_0I_0}(t_2,t_1)\{\mu_{gI_0'}\mu_{I_0g} e^{i(-\bar{U}_1+\Omega_{\rm v})(t_2-t_1)} + \mu_{gI_0}\mu_{I_0'g} e^{i(\bar{U}_1-\Omega_{\rm v})(t_2-t_1)}\}\Big]$$

Faraday Discussions Accepted Manuscript

View Article Online
DOI: 10.1039/C4FD00178H

where we have dropped the continuum state subscripts on the Green's functions since they are assumed to be independent of the nuclear coordinates. The $\bar{U}_{1(3)}$ are defined as before and

$$\bar{U}_5 \equiv \frac{1}{t_6 - t_5} \int_{t_5}^{t_6} dt' \mathcal{E}_{\tilde{I}_0 \to \tilde{I}_0'}(t') - \mathcal{E}_{I_1' \to I_1''}(\tau') \tag{58}$$

is the time-averaged gap, electronic energy gap between the core-hole states and the dicationic-valence states. Equations (55) and (57) must still be averaged over nuclear degrees of freedom. This may be performed, as in TRPES, by propagating the system along trajectories and averaging. The expressions are written so as to facilitate this approach.

VI. OFF-RESONANT X-RAY SCATTERING

X-ray scattering is commonly employed for monitoring the electronic and nuclear structure of materials [43–45]. In the resonant case, this leads to X-ray absorption spectroscopy as well as higher-order multidimensional techniques which are commonly employed to obtain information on the electronic structure and track the dynamics of wavepackets of nuclear excitations. In the off-resonant case, this leads to diffraction which is used to determine the static structure of complex systems as well as to monitor the motion of the nuclei in nonequilibrium processes (e.g. crystal melting [46, 47]).

In a recent work, we analyzed the scattering of off-resonant X-rays coupled to matter via the A^2 term in the minimal-coupling Hamiltonian and gave a unified treatment of time, frequency, and wavevector resolution through a rigorous incorporation of the photon-detection event [30]. The signal is taken to be the integrated field intensity at the detector

$$S_{\mathrm{OXS}}(\bar{\omega}, \bar{t}, \bar{\mathbf{r}}, \bar{\mathbf{k}}) = \int dt \int d\mathbf{r} \langle \mathbf{E}^{(t\mathbf{r}f\mathbf{k})\dagger}(\mathbf{r}, t) \mathbf{E}^{(t\mathbf{r}f\mathbf{k})}(\mathbf{r}, t) \rangle. \tag{59}$$

where the field superscripts indicate the multiplication (in appropriate domains) by detector gating functions and the arguments of the signal are the central parameters of these functions (we leave the dependence on the detector widths implicit). Since the detected field mode was initially unoccupied, we model the interaction as spontaneous emission into vacuum field modes (labeled with s, s') and reabsorption at the detector. The probe field (labeled with p, p') enters through the magnetic vector potential $\mathbf{A}$. Since the vector potential is linearly coupled to the system's charge density (labeled $\hat{\sigma}$), the bare OXS signal (before consideration of the detector effects) will come as

$$S_{\mathrm{OXS,B}}(t', \omega', \mathbf{r}', \mathbf{k}') \propto \sum_{ss'} \int d\mathbf{r}_1 d\mathbf{r}_1' \int dt_1 dt_1' \tag{60}$$
$$\langle\langle \mathbb{1} | \mathbf{E}_R^{(s')\dagger}(\mathbf{r}', t') \mathbf{E}_L^{(s)}(\mathbf{r}', t') \mathbf{A}_R^{(s')}(\mathbf{r}_1', t_1') \cdot \mathbf{A}_R^{(p)\dagger}(\mathbf{r}_1', t_1') \sigma_R(\mathbf{r}_1', t_1') \mathbf{A}_L^{(s)\dagger}(\mathbf{r}_1, t_1) \cdot \mathbf{A}_L^{(p)}(\mathbf{r}_1, t_1) \sigma_L(\mathbf{r}_1, t_1) | \rho_T(0) \rangle\rangle$$

where $|\rho_T(0)\rangle\rangle$ is the total (field and matter) density matrix at time 0 (taken to be the terminus of a process that leaves the system in a nonequilibrium state). This is illustrated diagramatically in fig. (5). The signal is not generally related to the time-dependent, single-particle momentum-space charge density but rather to its correlation function [27, 48]. A compact expression for the signal in the limit of ideal spatial and spectral detector resolution

$$S_{\mathrm{OXS}}(\bar{\omega}, \Lambda) \propto \int d\omega_p d\omega_{p'} E_p(\omega_p) E_p^*(\omega_{p'}) \langle \sigma_T(-\mathbf{q}', \omega_{p'} - \bar{\omega}) \sigma_T(\mathbf{q}, \bar{\omega} - \omega_p) \rangle \tag{61}$$

where $\mathbf{q}^{(\prime)} \equiv \frac{\bar{\omega}}{c} \hat{\bar{\mathbf{r}}} - \mathbf{k}_{p^{(\prime)}}$ is the momentum transfer (not to be confused with the nuclear coordinates of previous sections), $\hat{\bar{\mathbf{r}}}$ is the normalized position vector of the detector pixel relative to the sample center, and Λ represents the pulse parameters. Assuming that the sample is composed of N identical, non-interacting molecules (indexed by α, β), the correlation function of the total charge density operator (σ_T) may be expanded as

$$\langle \sigma_T(-\mathbf{q}', \omega - \omega_{p'}) \sigma_T(\mathbf{q}, \omega_p - \omega) \rangle = \tag{62}$$
$$\sum_\alpha e^{-i(\mathbf{q}-\mathbf{q}')\cdot\mathbf{r}_\alpha} \langle \sigma(-\mathbf{q}', \omega - \omega_{p'}) \sigma(\mathbf{q}, \omega_p - \omega) \rangle + \sum_\alpha \sum_{\beta \neq \alpha} e^{-i(\mathbf{q}\cdot\mathbf{r}_\alpha - \mathbf{q}'\cdot\mathbf{r}_\beta)} \langle \sigma(-\mathbf{q}', \omega - \omega_{p'}) \rangle \langle \sigma(\mathbf{q}, \omega_p - \omega) \rangle$$

where $\mathbf{r}_\alpha$ is the position vector of the center of particle α and we have taken $\hat{\sigma}_T(\mathbf{r}) = \sum_\alpha \hat{\sigma}(\mathbf{r} - \mathbf{r}_\alpha)$ so that the total charge density is composed of a superposition of the (identical) charge densities associated with each molecule (assumed to be non-overlapping). We classify the former (one-particle) terms in eq. (62) incoherent and the latter

Published on 04 November 2014. Downloaded by University of California - Irvine on 04/11/2014 18:23:19.
Faraday Discussions Accepted Manuscript

View Article Online
DOI: 10.1039/C4FD00178H

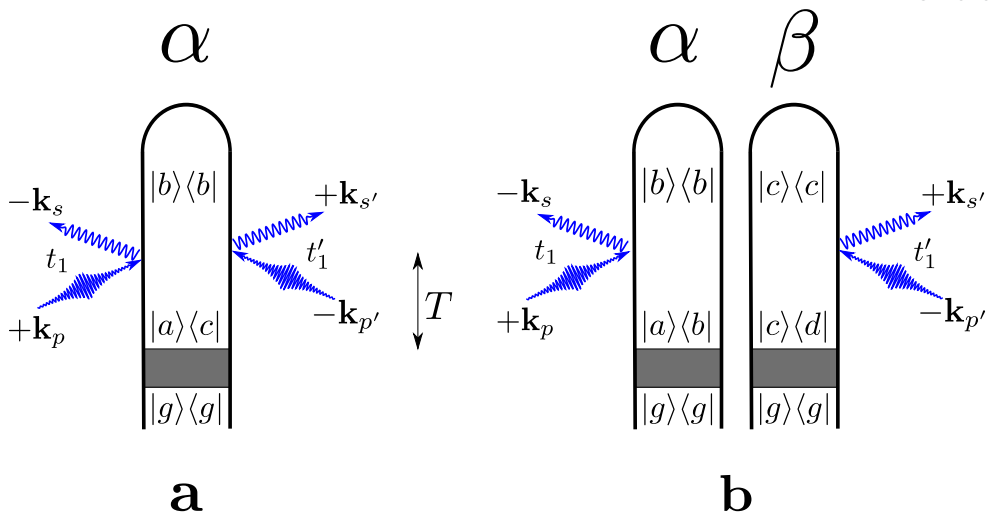

FIG. 5. Loop diagrams for incoherent (**a**) and coherent (**b**) X-ray scattering processes. The shaded area represents an unspecified process that prepares the system in an arbitrary state ($|g\rangle$ is the electronic ground state). We denote modes of the pump with p and p' whereas s, s' represent relevant scattering modes ($\mathbf{k}_{p^{(\prime)}}$ has frequency $\omega_{p^{(\prime)}}$ and $\mathbf{k}_{s^{(\prime)}}$ has frequency $\omega_{s^{(\prime)}}$). The time T between the termination of this preparation process and the central time of the scattered pulse is shown via the arrow in the center of the figure. Elastic scattering corresponds to $\omega_{ab} = \omega_{bc} = 0$ (i.e. $\omega_{ac} = 0$ for the incoherent and $\omega_{bc} = \omega_{ed} = 0$ for the coherent contribution. Elastic scattering therefore originates from scattering off populations. For diagram rules, see [52, 53]

(two-particle) terms coherent, reflecting the way in which contributions from different molecules in these terms add together. Of particular note is that these two contributions come with different form factors. The incoherent form factor permits excitation (inelastic scattering) from the ground state while the coherent form factor only permits transitions between previously occupied states and is therefore purely elastic when considering scattering from the ground state. This is clearly seen from fig. (5) since the coherent terms only have interactions on one side of the density matrix and therefore cannot cause transitions to unoccupied states.

Ordinarily, X-ray diffraction is elastic and comes as the Fourier Transform of the real-space charge density. Since the number of two-particle terms scales quadratically with the molecule number (versus the linear scaling of the one-particle terms), off-resonant scattering from the ground state is dominated by the elastic contribution. In the case of single-molecule samples or nonstationary initial states, the contribution from inelastic terms increases and can become substantial for certain values of $\mathbf{q}$. The inelasticities are therefore overwhelmed by the elastic contributions for many-particle samples but are important in analyzing single-molecule scattering patterns. In particular, the off-resonant X-ray scattering from a single molecule cannot be represented as the ground state momentum-space charge density as in ordinary diffraction experiments. It is for this reason that we avoid the use of the term diffraction (which could be taken to imply this form for the signal) in favor of the more generic "scattering". This gave rise to the possibility of creating a coherent excitation via off-resonant scattering and probing this excitation with a second pulse, a process termed multidimensional X-ray diffraction [49].

A future goal would be to introduce this level of theory to the detection event for photoelectron and Auger-electron experiments. This would require a quantum-field theoretical treatment of the continuum electrons but would facilitate the incorporation of propagation effects between the sample and detector. Such effects are necessary for a description of attosecond-resolution techniques such as the attosecond streak camera and the RABBIT technique [2, 50, 51].

VII. CONCLUSIONS

The electronic and nuclear structure and dynamics of molecules and materials are routinely probed by TRPES, AES, and OXS techniques. We have reported a Liouville-space description of these signals. The abundance of different degrees of freedom (core, valence, and continuum electronic states, vibrations, and solvent/environmental effects) is most easily handled in a Liouville-space framework since one may start with the full Liouvillian and approximate different degrees of freedom at different levels (retaining Hamiltonian evolution only for the fastest dynamics). For example, one can therefore treat the electronic states and any nuclear coordinates that cause conical intersections at

Published on 04 November 2014. Downloaded by University of California - Irvine on 04/11/2014 18:23:19.
Faraday Discussions Accepted Manuscript

View Article Online
DOI: 10.1039/C4FD00178H

the Hamiltonian level while treating the remaining vibrational modes and the environment as a bath (which can be approximated in a variety of ways [7]). Moreover, the explicit incorporation of the detection event given in our account of OXS can be extended to TRPES and AES using a quantum field description of the electrons. This would then allow the formalism to handle propagation effects between the material and the detector such as multiple scatterings and external field effects as employed in the streak camera and RABBIT techniques to gain time resolution. Finally, all of these techniques leave the material system in a nontrivial excited state that can be the object of further study via traditional nonlinear spectroscopic techniques. Since, in Liouville space, the system (described by the $|\rho\rangle\rangle$ vector) travels only forward in time, the processes can be regarded in a modular fashion and further interactions are easily added to describe the probing of ionic states resulting from TRPES/AES processes.

ACKNOWLEDGMENTS

The support of the Chemical Sciences, Geosciences, and Biosciences division, Office of Basic Energy Sciences, Office of Science, U.S. Department of Energy as well as from the National Science Foundation (grant CHE-1361516), and the National Institutes of Health (Grant GM-59230) is gratefully acknowledged. Kochise Bennett was supported by DOE.

Appendix A: Liouville Space

In Liouville space, we promote the density matrix ρ to a vector denoted by a double ket $|\rho\rangle\rangle$. For every Hilbert space operator O, we associate Liouville space operators O_L and O_R that indicate action on the ket or bra of the density matrix respectively:

$$\begin{aligned} O_L|\rho\rangle\rangle &\leftrightarrow O\rho \\ O_R|\rho\rangle\rangle &\leftrightarrow \rho O \end{aligned} \tag{A1}$$

where the symbol "$\leftrightarrow$" indicates equivalence between Liouville and Hilbert space expressions. Additionally, we define an associated Liouvillian for every Hamiltonian defined above:

$$\mathcal{L} \equiv H_- \equiv H_L - H_R \tag{A2}$$

This definition allows compact expressions for the commutations with the interaction Hamiltonians. In Hilbert space, operator expectation values are given by the trace of the operator product with the density matrix. The Liouville space analogy is

$$\langle\langle \mathbb{1}|O_L|\rho\rangle\rangle \leftrightarrow \mathrm{Tr}\left[O\rho\right] \tag{A3}$$

where, as shorthand for the trace operator, we have used

$$\langle\langle \mathbb{1}| \equiv \sum_i \langle\langle ii| \tag{A4}$$

with i indexing any complete basis.

Appendix B: Second Quantized Fermionic Description

In the main text, we left the description of the bound molecular states arbitrary In this section, we take some preliminary steps toward describing the states and operators used in the TRPES and Auger sections in a 2nd-quantized language in terms of the occupation numbers of the single-particle orbitals. Although this has already been done for the continuum states, we now examine the bound states in this manner as well. We will not specify a model for the Hamiltonian but will simply use this to clarify the form of the transition dipoles and the Auger decay operator. We index valence orbitals with l, m, n and the core orbitals with α, β. In this basis, the Hamiltonians for the interaction with the valence pump and ionizing X-ray pulse are

$$H_{\mathrm{v}}(t) = -E_{\mathrm{v}}(t) \sum_{mn} \mu_{mn} c_m^\dagger c_n + \mathrm{c.c.} \qquad H_{\mathrm{x}}(t) = -E_{\mathrm{x}}(t) \sum_{\mathbf{p}\alpha} \mu_{\mathbf{p}\alpha} c_{\mathbf{p}}^\dagger c_\alpha + \mathrm{c.c.} \tag{B1}$$

Published on 04 November 2014. Downloaded by University of California - Irvine on 04/11/2014 18:23:19.

Faraday Discussions Accepted Manuscript

View Article Online
DOI: 10.1039/C4FD00178H

The A-operator (which controls the Auger decay of the core hole) is a generalized Coulomb matrix element and comes as

$$A = \sum_{\mathbf{k}\alpha mn} A_{\mathbf{k}\alpha mn} c^\dagger_{\mathbf{k}} c^\dagger_\alpha c_m c_n + \text{c.c.} \tag{B2}$$

where

$$A_{\mathbf{k}\alpha mn} = \int d\mathbf{r} d\mathbf{r}' \phi_{\mathbf{k}}(\mathbf{r}) \phi_\alpha(\mathbf{r}') \frac{1}{|\mathbf{r}-\mathbf{r}'|} \phi_m(\mathbf{r}) \phi_n(\mathbf{r}') \tag{B3}$$

We may explicitly connect these to the forms given in the main text by supposing that we can construct the excited states from the ground state. We thus write

$$\begin{aligned} |I_0\rangle &= \sum_{mn} O_{I_o mn} c^\dagger_m c_n |g\rangle \\ |I_1\mathbf{p}\rangle &= \sum_{\alpha I_0} O_{I_1 \alpha I_0} c^\dagger_{\mathbf{p}} c_\alpha |I_0\rangle \\ |\tilde{I}_0 \mathbf{p}\mathbf{k}\rangle &= \sum_{\alpha} O_{\tilde{I}_0 \alpha mn I_1} c^\dagger_{\mathbf{k}} c^\dagger_\alpha c_m c_n |I_1\mathbf{p}\rangle \end{aligned} \tag{B4}$$

where the O coefficients are chosen to diagonalize the respective subspaces. With this we obtain the relationship between the transition dipoles and Auger elements in the two bases:

$$\begin{aligned} \mu_{I_0 g} &= \sum_{mn} O_{I_0 mn} \mu_{mn} \\ \mu_{\mathbf{p} I_1 I_0} &= \sum_{\alpha} O_{I_1 \alpha I_0} \mu_{\mathbf{p}\alpha} \\ A_{\mathbf{k}\tilde{I}_0 I_1} &= \sum_{\alpha mn} O_{\tilde{I}_0 \alpha mn I_1} A_{\mathbf{k}\alpha mn} \end{aligned} \tag{B5}$$

[1] A. Stolow, A. E. Bragg, and D. M. Neumark, Chem. Rev. **104**, 1719 (2004).
[2] M. Hentschel, R. Kienberger, C. Spielmann, G. A. Reider, N. Milosevic, T. Brabec, P. Corkum, U. Heinzmann, M. Drescher, and F. Krausz, Nature **414**, 509 (2001).
[3] L. J. P. Ament, M. van Veenendaal, T. P. Devereaux, J. P. Hill, and J. van den Brink, Rev. Mod. Phys. **83**, 705 (2011).
[4] P. Thibault and V. Elser, Annu. Rev. Cond. Mat. Phys. **1**, 237 (2010).
[5] H. Meyer, Annu. Rev. Phys. Chem. **53**, 141 (2002).
[6] G. A. Worth and L. S. Cederbaum, Annu. Rev. Phys. Chem. **55**, 127 (2004).
[7] S. Mukamel, *Principles of Nonlinear Optical Spectroscopy*, 1st ed. (Oxford University Press, USA, 1995).
[8] M. Seel and W. Domcke, J. Chem. Phys. **95**, 7806 (1991).
[9] M. Ohno and G. Wendin, J. Phys. B-At. Mol. Phys. **12**, 1305 (1979).
[10] D. M. Neumark, Annu. Rev. Phys. Chem. **52**, 255 (2001).
[11] M. Chen, X. Wang, Y. Yu, Z. Pei, X. Bai, C. Sun, R. Huang, and L. Wen, Appl. Surf. Sci. **158**, 134 (2000).
[12] H. Petek and S. Ogawa, Prog. Surf. Sci. **56**, 239 (1997).
[13] H. R. Hudock, B. G. Levine, A. L. Thompson, H. Satzger, D. Townsend, N. Gador, S. Ullrich, A. Stolow, and T. J. Martínez, J. Phys. Chem. A **111**, 8500 (2007).
[14] A. L. Thompson and T. J. Martínez, Faraday Discuss. **150**, 293 (2011).
[15] T. S. Kuhlman, W. J. Glover, T. Mori, K. B. Møller, and T. J. Martínez, Faraday Discuss. **157**, 193 (2012).
[16] B. P. Fingerhut, K. E. Dorfman, and S. Mukamel, J. Phys. Chem. Lett. **4**, 1933 (2013).
[17] B. McFarland, J. Farrell, S. Miyabe, F. Tarantelli, A. Aguilar, N. Berrah, C. Bostedt, J. Bozek, P. Bucksbaum, J. Castagna, *et al.*, Nat. Comm. **5** (2014).
[18] C.-M. Liegener, J. Chem. Phys. **79**, 2924 (1983).
[19] N. Ottosson, G. Öhrwall, and O. Björneholm, Chem. Phys. Lett. **543**, 1 (2012).
[20] R. Manne and H. Ågren, Chem. Phys. **93**, 201 (1985).
[21] C.-M. Liegener, Chem. Phys. Lett. **90**, 188 (1982).
[22] M. Ohno, Phys. Rev. B **58**, 12795 (1998).
[23] O. Gunnarsson and K. Schönhammer, Phys. Rev. B **22**, 3710 (1980).
[24] L. Cederbaum and W. Domcke, Adv. Chem. Phys. **36**, 205 (1977).

Published on 04 November 2014. Downloaded by University of California - Irvine on 04/11/2014 18:23:19.

Faraday Discussions Accepted Manuscript

View Article Online
DOI: 10.1039/C4FD00178H

[25] G. Wendin, *Breakdown of one-electron pictures in photoelectron spectra* (Springer, 1981).
[26] L. Hedin, J. Michiels, and J. Inglesfield, Phys. Rev. B **58**, 15565 (1998).
[27] W. Schulke, *Electron dynamics by inelastic X-ray scattering* (Oxford University Press, Oxford; New York, 2007).
[28] J. Als-Nielsen and D. McMorrow, *Elements of modern X-ray physics* (Wiley, Hoboken, 2011).
[29] C. Bressler and M. Chergui, Chem. Rev. **104**, 1781 (2004).
[30] K. Bennett, J. D. Biggs, Y. Zhang, K. E. Dorfman, and S. Mukamel, J. Chem. Phys. **140**, 204311 (2014).
[31] J. Hajdu, Curr. Opin. Struc. Biol. **10**, 569 (2000).
[32] D. Starodub, A. Aquila, S. Bajt, M. Barthelmess, A. Barty, C. Bostedt, J. Bozek, N. Coppola, R. Doak, S. Epp, *et al.*, Nat. Commun. **3**, 1276 (2012).
[33] H. N. Chapman, Nat. Mater. **8**, 299 (2009).
[34] H. N. Chapman, A. Barty, M. J. Bogan, S. Boutet, M. Frank, S. P. Hau-Riege, S. Marchesini, B. W. Woods, S. Bajt, and W. H. Benner, Nat. Phys. **2** (2006), 10.1038/nphys461.
[35] S. Rahav and S. Mukamel, Phys. Rev. A **81**, 063810 (2010).
[36] H.-J. Werner, P. J. Knowles, G. Knizia, F. R. Manby, and M. Schütz, WIREs Comput. Mol. Sci. **2**, 242 (2012).
[37] A. M. D. Lee, J. D. Coe, S. Ullrich, M. L. Ho, S. J. Lee, B. M. Cheng, M. Z. Zgierski, I. C. Chen, T. J. Martinez, and A. Stolow, J. Phys. Chem. A **111**, 11948 (2007).
[38] S. Hammes-Schiffer and J. C. Tully, J. Chem. Phys. **101**, 4657 (1994).
[39] M. Barbatti, M. Ruckenbauer, F. Plasser, J. Pittner, G. Granucci, M. Persico, and H. Lischka, WIREs Comput. Mol. Sci. **4**, 26 (2014).
[40] T. Mori, W. J. Glover, M. S. Schuurman, and T. J. Martinez, J. Phys. Chem. A **116**, 2808 (2011).
[41] C. M. Oana and A. I. Krylov, J. Chem. Phys. **127**, 234106 (2007).
[42] A. Perveaux, D. Lauvergnat, B. Lasorne, F. Gatti, M. A. Robb, G. J. Halász, and A. Vibók, J. Phys. B-At. Mol. Opt. Phys. **47**, 124010 (2014).
[43] R. Neutze, R. Wouts, D. van der Spoel, E. Weckert, and J. Hajdu, Nature **406**, 752 (2000).
[44] H. N. Chapman, P. Fromme, A. Barty, T. A. White, R. A. Kirian, A. Aquila, M. S. Hunter, J. Schulz, D. P. DePonte, and U. Weierstall, Nature **470**, 73 (2011).
[45] R. Koopmann, K. Cupelli, L. Redecke, K. Nass, D. P. DePonte, T. A. White, F. Stellato, D. Rehders, M. Liang, J. Andreasson, *et al.*, Nat. Methods **9**, 259 (2012).
[46] C. W. Siders, A. Cavalleri, K. Sokolowski-Tinten, C. Tth, T. Guo, M. Kammler, M. H. v. Hoegen, K. R. Wilson, D. v. d. Linde, and C. P. J. Barty, Science **286**, 1340 (1999).
[47] J. Larsson, R. W. Falcone, *et al.*, Appl. Phys. A Mater. Sci. Process. **66**, 587 (1998).
[48] M. J. J. Vrakking and T. Elsaesser, Nat. Photonics **6**, 645 (2012).
[49] J. D. Biggs, K. Bennett, Y. Zhang, and S. Mukamel, J. Phys. B-At. Mol. Opt. Phys. **47**, 124037 (2014).
[50] J. M. Dahlström, D. Guénot, K. Klünder, M. Gisselbrecht, J. Mauritsson, A. L'Huillier, A. Maquet, and R. Taïeb, Chem. Phys. **414**, 53 (2013).
[51] P. . M. Paul, E. Toma, P. Breger, G. Mullot, F. Augé, P. Balcou, H. Muller, and P. Agostini, Science **292**, 1689 (2001).
[52] K. E. Dorfman, K. Bennett, Y. Zhang, and S. Mukamel, Phys. Rev. A **87**, 053826 (2013).
[53] J. D. Biggs, J. A. Voll, and S. Mukamel, Phil. Trans. R. Soc. A **370**, 3709 (2012).

Published on 04 November 2014. Downloaded by University of California - Irvine on 04/11/2014 18:23:19.

Faraday Discussions Accepted Manuscript